



Epigallocatechin-3-gallate inhibits osteopontin expression and prevents experimentally induced hepatic fibrosis

Joseph George^{a,b,1,*}, Mutsumi Tsuchishima^{a,2}, Mikihiro Tsutsumi^{a,b,3}

^a Department of Hepatology, Kanazawa Medical University, Uchinada, Ishikawa 920-0293, Japan

^b Center for Regenerative Medicine, Kanazawa Medical University Hospital, Uchinada, Ishikawa 920-0293, Japan

ARTICLE INFO

Keywords:

Epigallocatechin-3-gallate
Osteopontin
N-Nitrosodimethylamine
Hepatic fibrosis
4-hydroxy-2-nonenal

ABSTRACT

Osteopontin (OPN) is a matricellular cytokine and a stress-induced profibrogenic molecule that promotes activation of stellate cells during the pathogenesis of hepatic fibrosis. We studied the protective effects of epigallocatechin-3-gallate (EGCG) to suppress oxidative stress, inhibit OPN expression, and prevent experimentally induced hepatic fibrosis. Liver injury was induced with intraperitoneal injections of N-nitrosodimethylamine (NDMA) in a dose of 1 mg/100 g body weight on 3 consecutive days of a week for 28 days. A group of rats received 0.2 mg EGCG/100 g body weight orally everyday during the study. The animals were sacrificed on day 28th from the beginning of exposure. Serum levels of AST, ALT, OPN, malondialdehyde, collagen type IV, and hyaluronic acid were measured. Immunohistochemistry and/or real-time PCR were performed for α -SMA, 4-HNE, OPN, collagen type I, and type III. Serial administrations of NDMA produced well developed fibrosis and early cirrhosis in rat liver. Treatment with EGCG significantly reduced serum/plasma levels of AST, ALT, OPN, malondialdehyde, collagen type IV, and hyaluronic acid and prevented deposition of collagen fibers in the hepatic tissue. Protein and/or mRNA levels demonstrated marked decrease in the expression of α -SMA, 4-HNE, OPN, collagen type I, and type III. Treatment with EGCG prevented excessive generation of reactive oxygen species, suppressed oxidative stress, significantly reduced serum and hepatic OPN levels, and markedly attenuated hepatic fibrosis. The results indicated that EGCG could be used as a potent therapeutic agent to prevent hepatic fibrogenesis and related adverse events.

1. Introduction

Hepatic fibrosis is the outcome of a continuous wound healing process to a chronic liver injury and is marked with increased synthesis and deposition of extracellular proteins, especially collagens in the liver [1–3]. The pathogenesis of hepatic fibrosis is a complex and dynamic process in response to a chronic stimuli such as steatosis, viral hepatitis, drugs, toxins, alcohol, cholestasis, and metabolic disorders [4,5]. The chronic stimuli responsible for the initiation of fibrosis leads to generation of reactive oxygen species (ROS) that triggers several molecular events involved in the process of fibrogenesis [6–8]. In addition, acute and chronic hypoxia could lead to hepatitis and activation of hypoxia-inducible factor (HIF), which in turn triggers nuclear factor kappa B (NF- κ B) that incite several signaling pathways [9,10]. These

processes results in cellular injury and increase the expression of a variety of inflammatory cytokines, chemokines, and growth factors that trigger activation and transformation of quiescent hepatic stellate cells into myofibroblast like cells [11,12]. The activated and transformed stellate cells rapidly proliferate and dramatically upregulate a number of genes for connective tissue proteins, especially collagens and start excessive synthesis and deposition of respective proteins in the extracellular matrix leading to fibrosis. [13,14]. Inhibition of the excessive generation of ROS and subsequent activation of hepatic stellate cells could arrest pathogenesis of hepatic fibrosis and further adverse events.

Osteopontin (OPN), also known as bone sialoprotein–1 (BSP1) or secreted phosphoprotein–1 (SPP1), was first cloned and sequenced in 1986 [15]. It is a multifunctional cytokine that plays a prominent role in development, innate immunity, cell proliferation, tumor invasion, and

* Corresponding author at: Department of Hepatology, Kanazawa Medical University, Uchinada, Ishikawa 920-0293, Japan.

E-mail address: georgej@kanazawa-med.ac.jp (J. George).

¹ ORCID: 0000-0001-5354-7884

² ORCID: 0000-0003-4634-5592

³ ORCID: 0000-0003-0463-074X

angiogenesis [16]. OPN is expressed in a variety of cells including fibroblasts, macrophages, dendritic cells, endothelial cells, and smooth muscle cells [17]. OPN is a key modulator of hepatic inflammation, steatosis, fibrosis, and cancer progression [18]. We have observed that OPN is a stress induced profibrogenic molecule that promotes activation of stellate cells during the pathogenesis of hepatic fibrosis and ROS can upregulate OPN both in vitro and in vivo [19]. Furthermore, we have noticed that OPN reflects the degree of hepatic fibrosis and serves as a biomarker in patients hepatitis C virus (HCV) infection [20].

Epigallocatechin-3-gallate (EGCG) is a polyphenol and a potent antioxidant abundantly present in dried leaves of green tea [21]. EGCG induces tumor cell apoptosis, has antiangiogenic and antitumor properties, and also act as a modulator of tumor cell response to chemotherapy [21]. It was observed that EGCG prevents oxidative stress, hepatic fat deposition, and infiltration of inflammatory cells in experimentally induced nonalcoholic steatohepatitis (NASH) in mice [22]. Furthermore, it was reported that EGCG protects against hepatic ischemia-reperfusion injury and apoptotic cell death by decreasing oxidative stress in a mouse model [23]. However, the effects of EGCG to suppress the expression of the profibrogenic cytokine OPN and its protective effects against the pathogenesis of hepatic fibrosis have not been evaluated.

We have demonstrated that *N*-nitrosodimethylamine (NDMA) induced model of liver injury and hepatic fibrosis in rats is a quick and reproducible animal model and is appropriate to study the early events associated with the pathogenesis of human hepatic fibrosis and alcoholic cirrhosis [24,25]. Furthermore, we have clearly elucidated the molecular mechanisms involved in the pathogenesis and development of NDMA-induced model of hepatic fibrosis and early cirrhosis [26,27]. In the present study, we investigated the antioxidant effects of EGCG to suppress the expression of OPN and subsequent protection against the development of hepatic fibrosis during serial administrations of NDMA in rats.

2. Materials and methods

2.1. Animals

Male albino rats of Wistar strain at the age of around three months and weighing between 250 and 300 g were used for the experiments. We have previously demonstrated that three months old young adult male rats without diseases are appropriate to study the biochemical events associated with the pathogenesis of hepatic fibrosis [28]. All the animals were maintained in an air-conditioned and humidity controlled animal house under 12-h light/12-h dark cycles with commercial rat feed pellets and water available ad libitum. All the animal experimental procedures were carried out with relevant guidelines and regulations and followed the *Guide for the Care and Use of Laboratory Animals* prepared by the National Academy of Sciences and published by the US National Institutes of Health (NIH Publication No. 86-23, revised 1996). The animal experiments protocol (# 2012-47) was approved by the Animal Care and Use Committee of Kanazawa Medical University on the Ethics and Use of Laboratory Animals. All the animal experiments were carried out in the animal house and associated laboratories of Kanazawa Medical University, Uchinada, Japan.

2.2. Experimental procedure

A total of 24 animals were used for the study. The animals were divided into 4 groups of six rats each. The first group served as healthy control and the second group as drug control (EGCG group). The third group used for induction of hepatic fibrosis (NDMA group) and the 4th group was to study the effect of EGCG to prevent the development of hepatic fibrosis (NDMA-EGCG group). Hepatic fibrosis was induced by serial intraperitoneal administrations of *N*-nitrosodimethylamine (NDMA) (#N7756; Mol Wt 74.08, density 1.01 g/ml, Sigma-Aldrich, St.

Louis, MO, USA) in a dose of 1 mg/100 g body weight (10 µl diluted to 1 ml with 0.15 mol/L sterile NaCl) on three consecutive days of a week over a period of four weeks [29]. Healthy control animals received sterile NaCl without NDMA. The course of the treatment, dosage of NDMA, and duration of the experiment have been standardized previously to develop well-formed fibrosis and early cirrhosis [30,31]. The 4th group of NDMA treated animals received EGCG at a dose of 0.2 mg/100 g body weight about 2 h prior to the administration of NDMA and at the same time on all the remaining days during the study. Drug control animals received the same dose of EGCG along with the NDMA treated group. The dosage was decided after trial experiments and based on previous reports [32]. EGCG is readily soluble in water and prepared at a concentration of 50 mg/100 ml. The drug was administered orally employing intragastric tefflon tubes (Cat #KN-349-RC; Natsume Seisakusho, Tokyo, Japan) at a dose of 1 ml/250 g body weight. Body weight and behavioral changes of the animals were monitored throughout the study. All the animals were sacrificed on day 28 from the beginning of exposure. The animals were anaesthetized with isoflurane and blood was collected from right jugular vein. Serum was separated and stored in polypropylene vials at -80°C until assayed. The liver was rapidly removed, washed in cold phosphate buffered saline, and weighed in the wet state after blotting off water. A median lobe of 3 mm thick was cut and instantly fixed in 10% phosphate-buffered formalin for histopathological studies. Another portion of the liver was frozen at -80°C for biochemical analyses.

2.3. Histopathological evaluation of the liver tissue after serial administrations of NDMA and treatment with EGCG

Hematoxylin and Eosin (H&E) and Azan trichrome staining was used to assess the development of hepatic fibrosis after serial administrations of NDMA and to evaluate the effect of treatment with EGCG. The paraffin-embedded tissues were cut into sections of 5 µm thick, deparaffinized, and hydrated. The serial sections were then stained for H&E and Azan trichrome as per the standard protocol. The stained sections were examined using an Olympus BX51 microscope (Olympus corporation, Tokyo, Japan) attached with an Olympus digital camera (DP71) and photographed.

2.4. Measurement of AST and ALT in serum

Aspartate transaminase (AST) and alanine transaminase (ALT) in the serum are potent markers of hepatic necrosis and impairment of liver. We measured AST and ALT levels in rat serum after the serial administration of NDMA and after treatment with EGCG using an auto-analyzer exclusively for animal samples. AST and ALT values are presented as International Units per liter ((IU/liter) of serum.

2.5. Determination of total collagen content in the liver

Total collagen content in the liver tissue was measured as a biochemical parameter to assess the degree of hepatic fibrosis. Collagen content was determined by estimating hydroxyproline, a characteristic imino acid present in collagen. To estimate hydroxyproline, exactly 50 mg of wet liver tissue was hydrolyzed in 5 ml of 6 N HCl in sealed glass tubes at 110°C for 16 hrs. The hydrolyzed samples were evaporated to dryness in a boiling water bath to remove acid, and the residue was dissolved in 5 ml of distilled water. It was then treated with activated charcoal, vortexed well, and filtered through Whatman No. 1 filter paper. Hydroxyproline content in the clear filtrate was measured as described before [3]. The total collagen content in the liver tissue was calculated by multiplying the hydroxyproline content with a factor of 7.46 as described previously [2].

2.6. Measurement of malondialdehyde, hyaluronic acid, and collagen type IV

Malondialdehyde (MDA) is a potent marker for elevated intracellular levels of ROS and subsequent oxidative stress. Malondialdehyde present in the plasma was determined as a measure of lipid peroxidation employing spectrofluorometric method as described before [8]. Fluorometric method eliminates the measurement of nonspecific colored products of thiobarbituric acid (TBA) reaction while using plasma samples. In brief, 50 μ l of plasma was diluted to 0.5 ml with normal saline and mixed with 4 ml of 3 mol/L sulfuric acid and 0.5 ml of 10% phosphotungstic acid. It was allowed to stand for 5 min at room temperature and then centrifuged at 3000 rpm for 10 min. The supernatant was discarded and the sediment was suspended in 2 ml of distilled water. Then 1 ml of 0.67% TBA reagent (prepared freshly by dissolving TBA in 50% glacial acetic acid with gentle warming) was added. A standard solution was prepared using 1 nmol of 1,1,3,3-tetramethoxypropane in 2 ml of distilled water and 1 ml of TBA reagent. It was heated at 95 °C for 60 min in a water bath to generate MDA. After cooling in ice-cold water, the TBA-MDA adduct was extracted in 5 ml of spectroscopic grade *n*-butanol. It was centrifuged at 3000 rpm for 10 min and 3 ml of the butanol layer was collected. The fluorescence intensity was measured on a Hitachi fluorescence spectrophotometer (model F-7000; Hitachi Koki, Tokyo, Japan) at an excitation of 515 nm and an emission of 553 nm. The data are presented as nmoles malondialdehyde formed/ml plasma.

Collagen type IV present in rat serum was determined using a chemiluminescence based ELISA kit (Cat# NBP2-75863; Novus Biologicals, Centennial, CO, USA). The assay was performed as per the manufacturer's instructions and the levels of collagen type IV are presented as ng/ml serum. Hyaluronic acid (HA) concentrations in rat serum were determined using a Solid Phase Sandwich ELISA kit (Cat# DHYAL0; R&D Systems, Minneapolis, MN, USA) following the manufacturer's protocol. Serum HA levels are presented as ng/ml.

2.7. Measurement of osteopontin in serum

Serum levels of osteopontin (OPN) markedly increase during pathogenesis of hepatic fibrosis and its concentration is directly correlates with the degree of liver fibrosis [20]. In the current study, we measured serum levels of OPN after serial administrations of NDMA and treatment with EGCG using a rat OPN solid phase sandwich ELISA kit (Cat# 27360; Immuno-Biological Laboratories (IBL), Gunma, Japan) according to manufacturer's instructions. In brief, the serum samples were diluted 10 fold with the EIA buffer provided in the kit. Recombinant rat OPN ranging from 0 to 4.75 ng/ml was used as standards. Exactly, 100 μ l of diluted serum sample or standard solution was added to a microplate pre-coated with anti-rat OPN rabbit IgG, covered with the plate lid, and incubated for 60 min at 37 °C with gentle shaking. All test samples and standards were prepared in triplicate. Discarded the liquid, washed the wells five times with the wash buffer, and snapped the plate on Whatman paper. Then 100 μ l of HRP conjugated-second antibody was added and incubated at 4 °C for 30 min. The microplate was washed for six times, 100 μ l of TMB solution was added, and incubated exactly for 30 min at room temp in dark. The reaction was stopped by addition of 100 μ l of stop solution (1 N H₂SO₄) and the absorbance was measured within 10 min on a microplate reader at 450 nm. A standard curve was prepared using Microsoft Excel software in log-log mode and plotted a linear graph. The concentration of OPN in unknown samples was calculated from the regression equation obtained from the curve.

2.8. Immunohistochemical staining for α -smooth muscle actin, 4-HNE, and osteopontin

The expression of α -smooth muscle actin (α -SMA) is a characteristic and very specific marker for activated hepatic stellate cells. Reactive oxygen species (ROS) are involved in lipid peroxidation and membrane

lipids are one of the major targets of ROS. A variety of aldehydes are formed during peroxidation of membrane lipids and 4-hydroxy-2-nonenal (4-HNE) is an α , β -unsaturated aldehyde and one of the most reliable biomarkers of lipid peroxidation. The immunohistochemical staining for α -SMA, 4-HNE, and osteopontin was carried out on paraffin-embedded liver sections using a broad-spectrum histostain-plus kit (Invitrogen, Carlsbad, CA, USA). The paraffin liver sections were deparaffinized and hydrated to water. The slides for osteopontin staining were immersed in deionized water in a glass beaker and autoclaved at 121 °C for 20 min. After blocking, the clear liver sections were treated with primary antibodies against α -SMA (Cat# 412021; Nichirei Biosciences, Tokyo, Japan) or 4-HNE (Cat# HNE-J2; Nikken Seil, Shizuoka, Japan) or osteopontin (Cat# ab63856; Abcam, Chuo-ku, Tokyo, Japan) and incubated overnight in a moisturized chamber (Evergreen Scientific, Los Angeles, CA, USA) at 4 °C overnight. The sections were then washed 3–5 times with PBS and incubated with broad-spectrum biotinylated secondary antibody for 2 h at room temperature. The slides were again washed, treated with streptavidin-peroxidase conjugate, and incubated for another 1 h. The final stain was developed by using 3% 3-amino-9-ethylcarbazole (AEC) in N,N-dimethylformamide. The stained sections were washed and counterstained with Mayer's haematoxylin for 2 min and mounted using aqueous-based mounting medium. The dried slides were examined under a microscope (Olympus BX51, Tokyo, Japan) attached with a digital camera (Olympus DP71) and photographed. The images were quantified using Image-Pro Discovery software (Media Cybernetics, Silver Spring, MD, USA) and the data are presented as percentage square microns.

2.9. Quantitative real-time PCR for markers of hepatic fibrosis

In order to examine the upregulation of major molecular markers of hepatic fibrosis, we performed quantitative real-time PCR to evaluate mRNA levels of α -SMA, OPN, collagen type I, and collagen type III in the liver tissue following serial administrations of NDMA and after treatment with EGCG. Small pieces of liver tissue were flash frozen in liquid nitrogen and stored at – 80 °C. Total RNA was isolated from the frozen liver tissue employing PureLink RNA Mini Kit (Cat# 12183018A, Invitrogen, Carlsbad, CA, USA) in combination with Trizol (Cat# 15596026, Thermo Fisher, Waltham, MA, USA) as per manufacturer's instructions. The gene specific primers for α -SMA, OPN, collagen type I (α 1 chain), collagen type III (α 1 chain) and GAPDH were designed using Beacon Designer software (Premier Biosoft International, Palo Alto, CA). Details of the primer sets used are provided in supplementary Table 1. The cDNA was synthesized with 1–2 μ g of isolated total RNA using Prime-Script 1st strand cDNA Synthesis Kit (Cat# 6110 A, Takara Bio, Shiga, Japan) in a total volume of 20 μ l in RNase-free dH₂O at 42 °C for 60 min.

Real-time quantitative PCR (qPCR) was carried out with PowerTrack SYBR Green Master Mix (Cat# A46012, ThermoFisher, Waltham, MA, USA) on ABI 7900HT Fast Real-Time PCR System (Applied Biosystems, Foster City, CA). The synthesized cDNA was diluted to 20 fold with RNase-DNase-free water. The qPCR reaction was carried out with 5 μ l of diluted cDNA, 10 μ l of PowerTrack SYBR Green Master Mix, and nuclease free water containing gene specific primers and the Yellow sample buffer to a total volume of 20 μ l in a 384 well plate. All samples were run in triplicates. The qPCR machine was run on standard cycling mode and the parameters were set as, enzyme activation at 95 °C for 2 min (1 cycle), denature at 95 °C for 15 s and anneal/extend at 60 °C for 60 s (40 cycles). All data were normalized to GAPDH gene.

2.10. Isolation and culture of hepatic stellate cells and staining for osteopontin

In order to study whether stellate cells express OPN during pathogenesis of hepatic fibrosis, we stained cultured primary hepatic stellate cells for OPN. Stellate cells were isolated from adult albino rat liver, purified, characterized, and cultured as reported before [12]. About

Table 1

Sequences of the primers used in real-time RT-PCR.

Transcript	Genebank Number	Primer Sequence	Position	Length (m)	Product size (bp)
α -SMA	X13297	5'-CTGACAGAGGCACCACTGAA-3'	368F	20	160
		5'-CATCTCCAGAGTCCAGCACA-3'	527R	20	
Osteopontin	M14656	5'-ATGCTATCGACAGTCAGGCG-3'	864F	20	437
		5'-TGCAGTGGCCATTGCAATT-3'	1274R	20	
Collagen Type I (α 1)	BC059281	5'-AAGAGGCGAGAGGTTTCC-3'	2101F	20	244
		5'-AGAACCATCAGCACCTTTGG-3'	2344R	20	
Collagen Type III (α 1)	BC087039	5'-TGCAATGTGGGACCTGGTTT-3'	118F	20	501
		5'-GATAGCCACCCATTCTCCG-3'	618R	20	
GAPDH	BC145810	5'-AACTTTGGCATTGTGAAGG-3'	536F	20	223
		5'-ACACATTGGGGGTAGGAACA-3'	758R	20	

F: forward primer; R: reverse primer

80% confluent cells were sub-cultured into 4-well glass microscopic chamber slides (CAT# 154526PK, Lab-Tek, Thermo Fisher Scientific, Waltham, MA, USA) that are treated with 0.1% collagen solution. After 72 hrs, the media was discarded, washed the slides twice with PBS, and the cells were fixed in 1:1 methanol and ethanol mixture at -20°C for 10 min. The cells were washed with PBS and stained for α -SMA and OPN employing the respective antibodies used for paraffin sections. The cells are also stained for α -SMA in addition to OPN to demonstrate that all cultured cells express α -SMA, which is a characteristic marker for activated stellate cells.

2.11. Data analysis and statistics

All declared group size is the number of independent values and all statistical analyses were done on the independent values. Arithmetic mean and standard deviation were calculated for all the numerical data and presented as Mean \pm SD. The data were statistically analyzed using one-way analysis of variance (ANOVA) to evaluate the effect of EGCG treatment to ameliorate NDMA induced hepatic fibrosis. Least significant difference method was used to compare the mean values of NDMA group with NDMA-EGCG group. A value of $P < 0.05$ was considered statistically significant.

3. Results

3.1. Histopathological evaluation of hepatic fibrosis and effect of EGCG treatment

The histopathological evaluation of NDMA-induced hepatic fibrosis and the effect of EGCG treatment are depicted in Fig. 1A along with the respective controls. The control livers showed normal lobular architecture with central veins and radiating hepatic cords. Treatment with EGCG alone did not produce any histopathological changes in the rat liver. Serial administrations of NDMA produced well developed fibrosis with deposition of collagen fibers (arrow) in the hepatic parenchyma. There were infiltration of mononuclear cells and bridging fibrosis between central veins and portal triads. However, all these changes were either significantly reduced or absent in the livers treated with EGCG during the serial administrations of NDMA. Such livers depicted only mild to moderate focal hemorrhagic necrosis of hepatocytes with infiltration of mononuclear cells. The normal lobular hepatic architecture was almost intact.

Serum levels of AST and ALT in NDMA treated animals and also after the concurrent treatment with NDMA and EGCG are presented in Fig. 1B. Treatment with EGCG alone did not alter either AST or ALT level in the serum. Both AST and ALT levels were remarkably increased in the animals after the serial administrations of NDMA. Treatment with EGCG during NDMA administrations resulted in marked decrease of both AST and ALT levels.

3.2. Treatment with EGCG prevented deposition of collagen in the liver and reduced total collagen content

Azan trichrome staining is specific for connective tissue to demonstrate excessive synthesis and deposition of collagen fibers in the hepatic parenchyma during fibrogenesis. Azan staining did not show any collagen deposition in the hepatic parenchyma either in the control liver or livers treated EGCG alone (Fig. 2A). The four week course of serial administrations of NDMA produced well developed fibrosis and early cirrhosis with marked deposition of mature collagen fibers that stained in blue (arrows) (Fig. 2A). Simultaneous treatment with EGCG prevented hepatic fibrosis and deposition of collagen fibers in the hepatic parenchyma except the formation of thin collagen fibers between central vein and portal tracts.

The total collagen content in the liver tissue was measured to assess the increase of collagen in NDMA-induced hepatic fibrosis and to evaluate the effect of EGCG to prevent deposition of collagen in the liver. The total collagen content in the liver tissue was increased over 4-fold in NDMA treated animals compared to untreated controls (Fig. 2B). Concurrent administration of EGCG markedly reduced ($P < 0.001$) hepatic collagen content compared to the animals treated with NDMA alone (Fig. 2B).

3.3. EGCG decreased oxidative stress and lipid peroxidation

Malondialdehyde (MDA) is one of the final products of peroxidation of polyunsaturated fatty acids in the cells. An increase in free radicals causes overproduction of MDA. Increased levels of MDA indicate cellular oxidative stress and elevated lipid peroxidation. Plasma levels of MDA in NDMA induced hepatic fibrosis and after the treatment with EGCG is presented in Fig. 3A. The mean MDA level in plasma was markedly increased in the NDMA group compared to untreated controls. Concurrent treatment with EGCG during NDMA administrations resulted in significant reduction of MDA levels in serum (Fig. 3A). Treatment with EGCG alone did not produce any alteration of plasma MDA in the EGCG group.

3.4. EGCG treatment decreased hyaluronic acid and collagen type IV in serum

Serum HA is a very early indicator of toxic liver injury and hepatic fibrosis [30]. Serum type IV collagen used as a fibrogenesis marker in alcoholic liver disease and several other chronic liver injury [33]. Therefore, we measured serum concentrations of both HA and collagen type IV as biochemical markers of hepatic fibrosis and the data are presented in Fig. 3B and C, respectively. Both serum HA and collagen type IV concentrations are increased markedly after serial administrations of NDMA, which are well established factors in any type of chronic liver injury and hepatic fibrosis. Simultaneous treatment with EGCG during serial administrations of NDMA resulted in significant decrease

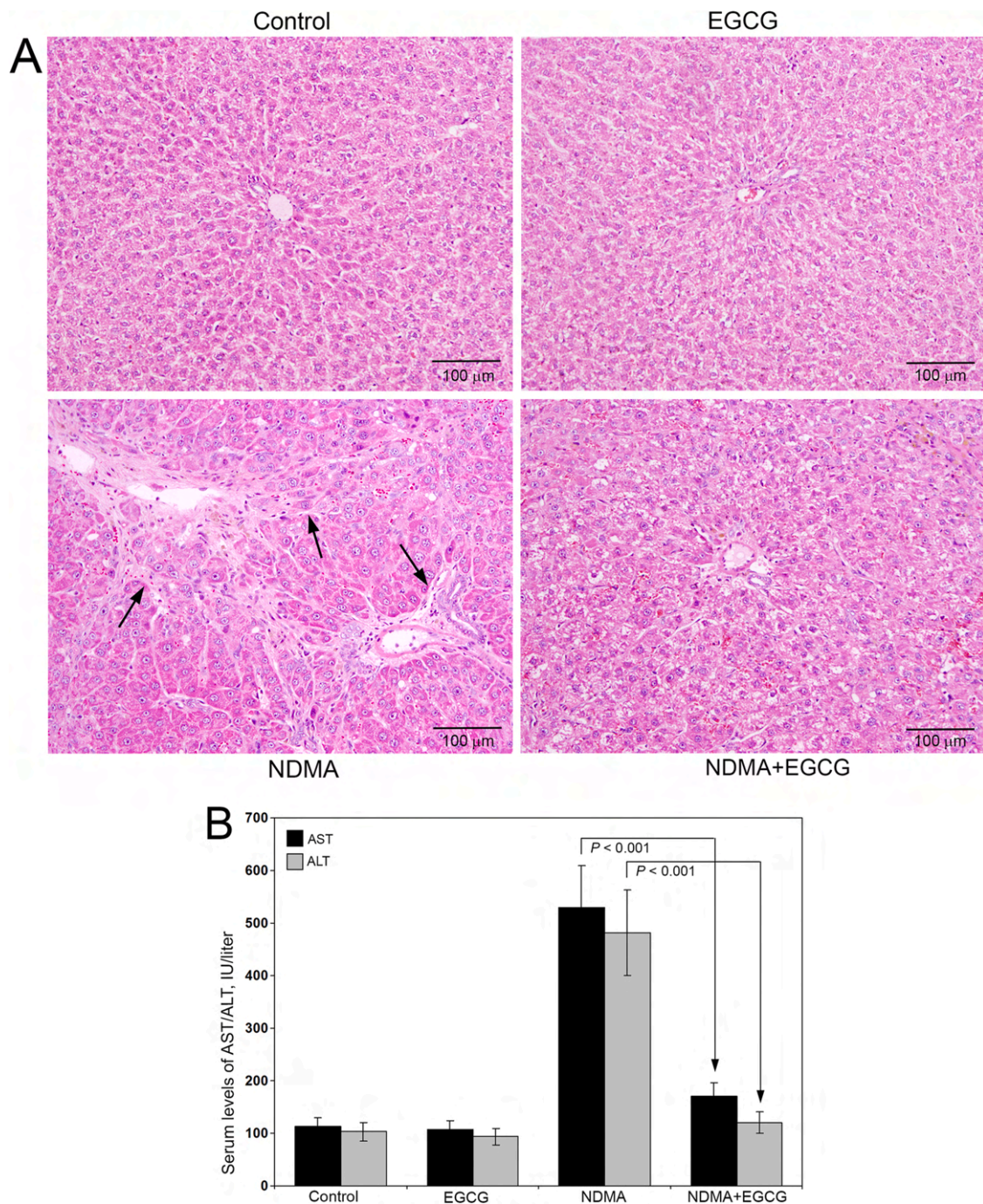


Fig. 1. (A) Hematoxylin and Eosin staining of rat liver sections following serial administrations of NDMA and after the treatment with EGCG. There were no histopathological alterations in the control and the livers treated with EGCG only. Serial intraperitoneal injections of NDMA produced well developed fibrosis and early cirrhosis with deposition of mature collagen fibers (arrows). Treatment with EGCG completely prevented liver fibrosis and deposition of collagen fibers in the hepatic parenchyma. Original magnification, $\times 100$. (B) Aspartate transaminase (AST) and alanine transaminase (ALT) levels in the serum following the administration of NDMA and after the treatment with EGCG. Treatment with EGCG resulted in significant reduction of serum AST and ALT levels following NDMA administration. The data are mean \pm S.D. of 6 rats in per group.

of both serum HA and collagen type IV, indicating the potent effect of EGCG to prevent hepatic fibrosis.

3.5. Treatment with EGCG markedly reduced serum osteopontin levels

Increased levels of serum OPN is a potent marker of hepatic fibrosis. However, serum OPN levels will increase in several pathological conditions including various cancers. The serum OPN concentrations measured using ELISA after NDMA-induced hepatic fibrosis and

concurrent treatment with EGCG are presented in Fig. 3D. A dramatic increase in serum OPN level was observed after the serial administrations of NDMA (Fig. 6D). Concurrent administration of EGCG resulted in marked decrease ($P < 0.001$) of mean serum OPN concentration in NDMA-EGCG group of animals. There was no difference in mean serum OPN concentrations between control and EGCG group.

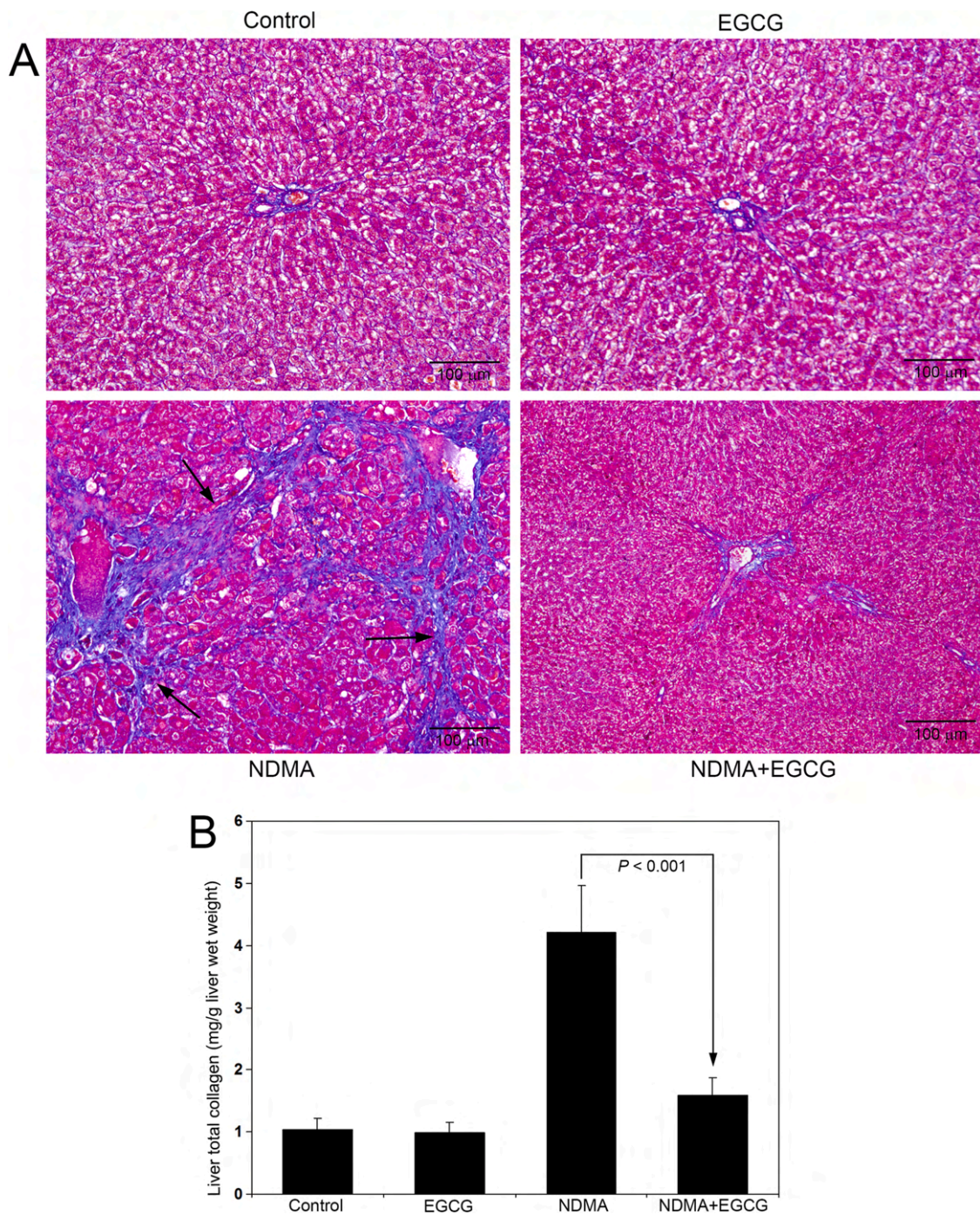


Fig. 2. (A) Azan trichrome staining for collagen in rat liver sections following serial administrations of NDMA and after the treatment with EGCG. There was no staining for collagen in the control and the livers treated with EGCG alone except in the central vein wall. Serial administrations of NDMA produced well developed fibrosis and early cirrhosis with the deposition of thick and mature collagen fibers stained in blue (arrows). Concurrent treatment with EGCG prevented liver fibrosis and deposition of collagen fibers in the hepatic parenchyma. However, mild collagen fibril formation was present between central vein and portal tracts. Original magnification, $\times 100$. (B) Total collagen content in the liver following the administration of NDMA and after concurrent treatment with EGCG. The data are mean \pm S.D. of 6 rats in per group.

3.6. Treatment with EGCG inhibited activation of hepatic stellate cells

Expression of α -SMA is considered as a marker for the activation of quiescent hepatic stellate cells in conjunction with the initiation of liver fibrosis [13]. Immunohistochemical staining was performed for α -SMA to examine the activation of hepatic stellate cells after the serial administrations of NDMA to induce hepatic fibrosis in rat liver. Staining for α -SMA was completely absent in the hepatic parenchyma of control

animals and the animals treated with EGCG alone (Fig. 4A). Remarkable and strong staining for α -SMA was in present in the fibrotic zone of rat livers treated with NDMA (arrows) indicating extensive activation of hepatic stellate cells (Fig. 4A). The staining for α -SMA was dramatically reduced in the rat livers concurrently treated with EGCG (Fig. 4A). Quantification of the staining intensity of α -SMA is presented as percentage square microns in Fig. 4B. The data indicated that the overall staining intensity of α -SMA has been decreased about 5-fold after the

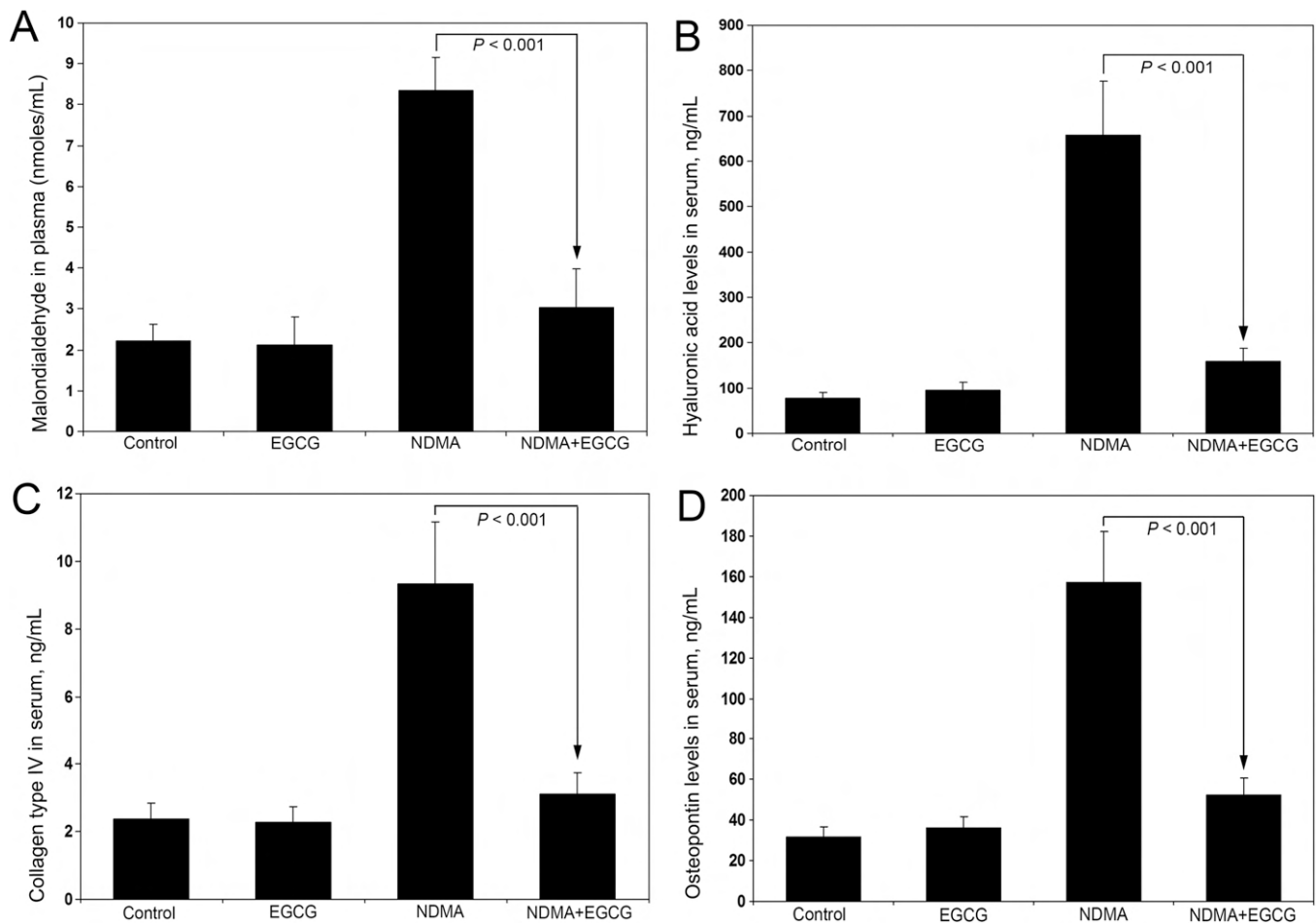


Fig. 3. Biochemical markers of hepatic fibrosis and the effect of EGCG treatment (A) Malondialdehyde levels in plasma. (B) Hyaluronic acid levels in serum. (C) Collagen type IV in serum. (D) Osteopontin in serum. All the parameters evaluated were significantly decreased after the treatment of EGCG. The data are mean \pm S. D. of 6 rats in per group.

concurrent treatment of EGCG during serial administrations of NDMA.

3.7. EGCG diminished production of 4-HNE

Excessive production and elevated levels of cellular ROS results in oxidative stress that leads to lipid peroxidation and formation of a variety of aldehydes. 4-Hydroxy-2-nonenal is an α,β -unsaturated aldehyde formed from the peroxidation of omega-6 unsaturated fatty acids such as linoleic acid and arachidonic acid [34]. The results of the immunohistochemical staining for 4-HNE in NDMA and EGCG treated animals are presented in Fig. 5A. Staining for 4-HNE was completely absent in control livers and animals treated with EGCG alone. Marked and conspicuous staining of 4-HNE was present in NDMA treated animal livers, especially in the necrotic and fibrotic zone (arrows) (Fig. 5A). On the other hand, only moderate staining of 4-HNE was present in the fibrotic zone in the animal livers concurrently treated with EGCG. Quantification of the staining intensity of 4-HNE is presented as percentage square microns in Fig. 5B. The staining intensity of 4-HNE was significantly reduced ($P < 0.001$) in NDMA-EGCG group compared to NDMA group.

3.8. Treatment with EGCG inhibited expression of osteopontin

Osteopontin is a stress sensitive profibrogenic cytokine that promotes activation of stellate cells during the pathogenesis of hepatic fibrosis. Immunohistochemical staining for OPN was performed in the liver tissue to examine the upregulation of OPN during pathogenesis of hepatic fibrosis and to study the effect of EGCG to prevent OPN

expression. Staining for OPN was absent in the paraffin liver sections of control and the animals treated with EGCG alone except a mild staining surrounding central vein and portal triads (Fig. 6A). Obvious and marked staining for OPN was present in the fibrotic areas of rat livers treated with NDMA (arrows) indicating increased expression of OPN during pathogenesis of hepatic fibrosis (Fig. 6A). Staining for OPN was significantly reduced in rat livers that are simultaneously administered EGCG along with NDMA (Fig. 6A). The outcome of quantitative analysis of the intensity of OPN staining employing Image-Pro Discovery software is depicted as percentage square microns in Fig. 6B. The data indicated that the staining for OPN was reduced significantly ($P < 0.001$) after the treatment with EGCG during serial administrations of NDMA to induce hepatic fibrosis.

3.9. Treatment with EGCG decreased expression of major molecules involved in hepatic fibrosis

The mRNA levels of α -SMA, OPN, collagen type I, and collagen type III were quantified in the liver tissue using real-time PCR in order to evaluate the enhanced expression during pathogenesis of hepatic fibrosis and to study the protective effect of EGCG to prevent the increase of those molecules during fibrogenesis. The rate of expression of mRNA of all the molecules examined were normalized to GAPDH gene and presented in Fig. 7. There was dramatic increase in the expression of all the molecules studied after the serial administrations of NDMA. The maximum increase (8.2 fold) was observed with regard to collagen type I followed by collagen type III in NDMA treated group. All the molecules

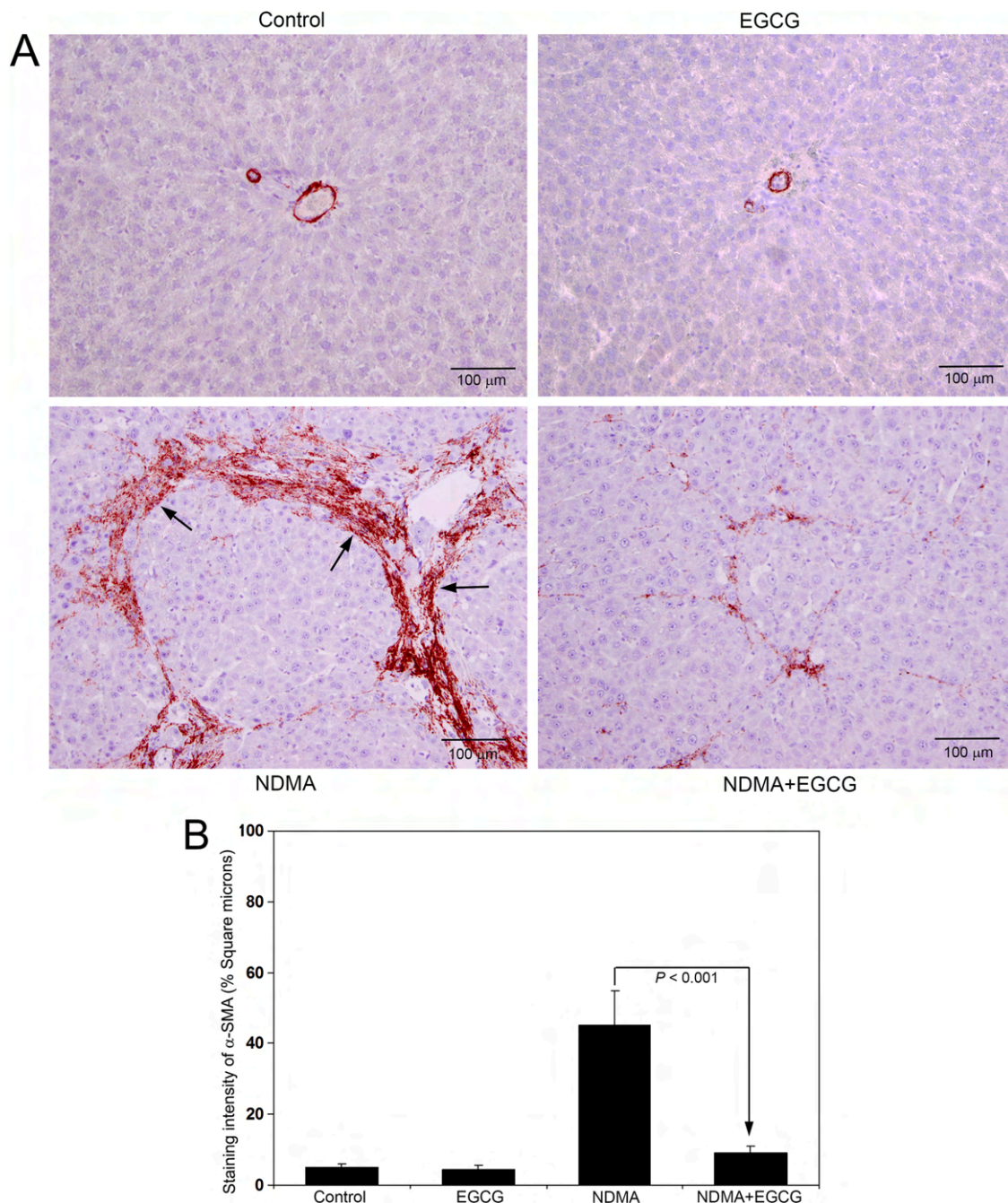


Fig. 4. (A) Immunohistochemical staining of α -smooth muscle actin (α -SMA) in rat liver sections following serial administrations of NDMA and after the treatment with EGCG. Staining for α -SMA was completely absent in the control and the livers treated with EGCG alone. Remarkable staining for α -SMA was present in the fibrotic areas of rat livers treated with NDMA (arrows). The staining for α -SMA was markedly reduced after concurrent treatment with EGCG. Original magnification, $\times 100$. (B) Quantification of the staining intensity of α -SMA as square microns. The staining intensity was analysed using Image-Pro Discovery software. The data are mean \pm S.D. of 10 randomly selected microscopic fields from six rats per group.

studied were significantly reduced ($P < 0.001$) after the concurrent administration of EGCG indicating its protective effect to prevent the upregulation of the markers of hepatic fibrosis. It is important to note that mRNA levels of both collagen type I and type III were markedly reduced after the treatment with EGCG.

3.10. Activated hepatic stellate cells express osteopontin

Since OPN expression is dramatically increased in hepatic fibrosis, we isolated and cultured hepatic stellate cells from rat liver to study whether stellate cells express OPN during pathogenesis of hepatic

fibrosis. The results of the immunohistochemical staining for α -SMA and OPN is presented in Fig. 8A and B, respectively. The staining for OPN in the activated stellate cells in cultures was very strong and deep. The cells were stained for α -SMA also to demonstrate that all cultured cells express α -SMA, which is a characteristic marker for activated stellate cells.

4. Discussion

Hepatic fibrosis and alcoholic cirrhosis are major health problems with significant morbidity and mortality that affects several millions of people worldwide. It is characterized by excessive synthesis and

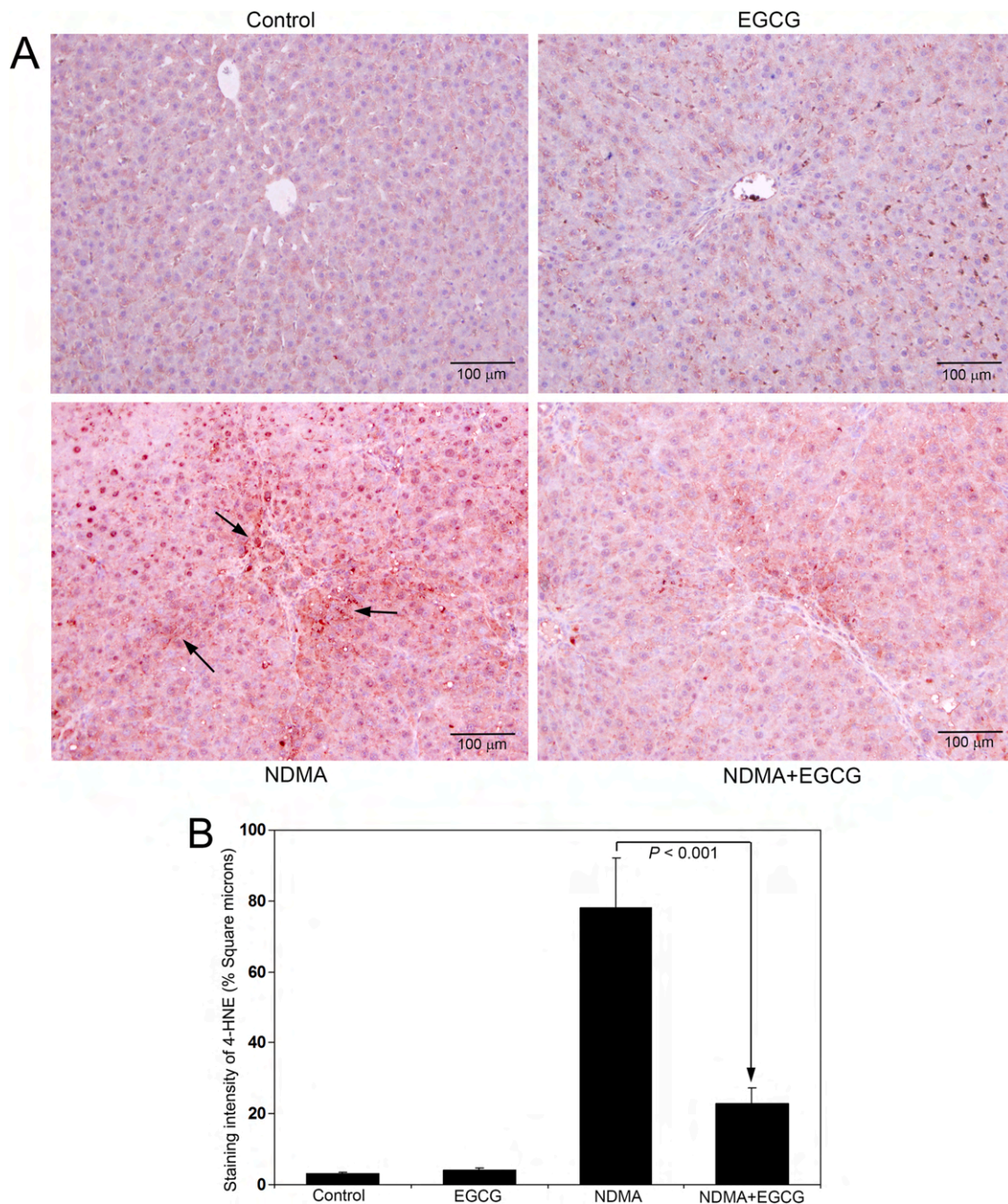


Fig. 5. (A) Immunohistochemical staining of 4-hydroxy-2-nonenal (4-HNE) in rat liver sections following serial administrations of NDMA and after the treatment with EGCG. Staining for 4-HNE was absent in the control and the livers treated with EGCG only. Marked staining for 4-HNE was present in the rat livers treated with NDMA (arrows). However, only mild staining was present in the livers treated with EGCG along with NDMA. Original magnification, $\times 100$. (B) Quantification of the staining intensity of 4-HNE. The staining intensity of 4-HNE was analysed employing Image-Pro Discovery software. The data are mean \pm S.D. of 10 randomly selected microscopic fields from six rats per group.

deposition of connective tissue proteins, especially interstitial collagens in the extracellular matrix of the liver. Clinical and experimental data indicate that excessive generation of reactive oxygen species (ROS) and subsequent cellular oxidative stress mediate the initiation and progression of liver fibrosis. It is well established that EGCG from green tea is a potent antioxidant that can prevent several diseases including pulmonary fibrosis and cancers [35]. EGCG is a polyphenol catechin with a molecular weight of 458.37 and having eight hydroxyl groups ($-\text{OH}$), which are important for the antioxidant activities to bind and detoxify free radicals [36]. EGCG is abundant in dried leaves of green tea (7380 mg per 100 gm) and 100 ml of green tea contains about 70 mg of

EGCG. Excessive intake of EGCG may induce hepatic toxicity and the recommended daily intake is about 700 mg when consumed as tea beverage and 338 mg as capsule [37]. Once the green tea turns into brown color, oxidation takes place and the number of available hydroxyl groups to bind with the free radicals will decrease.

Osteopontin is a multifunctional cytokine involved in various physiological and pathological process including inflammation, fibrogenesis, angiogenesis, and tumor progression [38]. Excessive generation of ROS and the resultant cellular oxidative stress occurs under several physiological and pathological conditions [39]. Metabolic interactions of drugs occur during multidrug therapy which cause upregulation of several

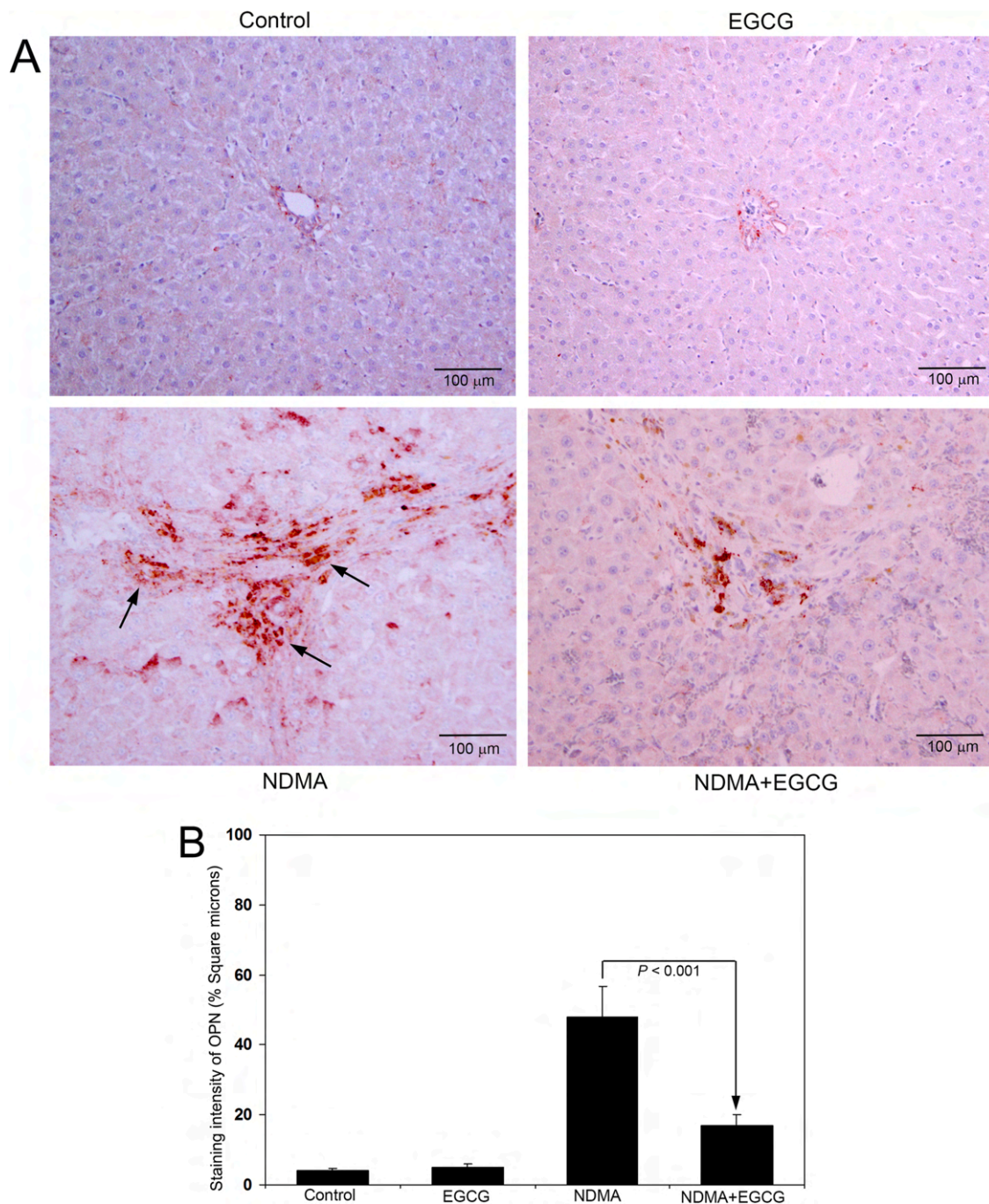


Fig. 6. (A) Immunohistochemical staining of osteopontin (OPN) in rat liver sections following serial administrations of NDMA and after the treatment with EGCG. Staining for OPN was absent in the control and the livers treated with EGCG alone. Conspicuous staining for OPN, especially in the fibrotic areas was present in the rat livers treated with NDMA (arrows). The staining for OPN was markedly reduced during concurrent treatment with EGCG. Original magnification, $\times 100$. (B) Quantification of the staining intensity of OPN. The staining intensity was analysed using Image-Pro Discovery software and presented as square microns. The data are mean \pm S.D. of 10 randomly selected microscopic fields from six rats per group.

cytochrome P450 subfamily of drug metabolizing enzymes that cause lipid peroxidation and excessive generation of ROS [40,41]. Osteopontin is highly upregulated during oxidative stress which in turn stimulates activation of hepatic stellate cells and promotes pathogenesis of hepatic fibrosis [19]. We have reported that in patients serum OPN levels coincide with the degree of hepatic fibrosis and can be used as a biomarker to assess the stage of fibrosis, which will help to reduce the number of liver biopsies [20]. In the current study, we have noticed a dramatic increase of serum and hepatic OPN levels, which were markedly reduced in EGCG treated animals. Both immunohistochemistry and

qPCR clearly demonstrated remarkable reduction of hepatic OPN expression in EGCG treated samples. These data indicate that EGCG binds with free radicals and ROS which in turn inhibits the upregulation of OPN and prevents progression of hepatic fibrosis. The metabolic degradation of NDMA by CYP2E1 produces extensive amounts of free radicals and ROS in the hepatic system and the resultant oxidative stress is responsible for the pathogenesis of hepatic fibrosis during NDMA administration.

Hepatic inflammation, repeated wound healing process, distortion of lobular architecture, and deposition of connective tissue components in

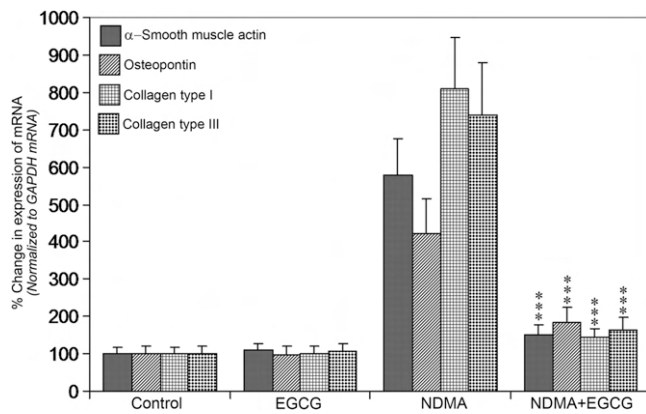


Fig. 7. Real-time quantitative PCR for the expression of α -SMA, OPN, collagen type I, and type III in rat liver following serial administrations of NDMA and after the treatment with EGCG. There was a dramatic increase in the expression of all the molecules studied which were markedly decreased in EGCG treated group. All the data are normalized to GAPDH mRNA that serve as housekeeping gene. The data are mean \pm S.D. of 6 rats in per group. *** $P < 0.001$ NDMA treated group versus NDMA+EGCG group.

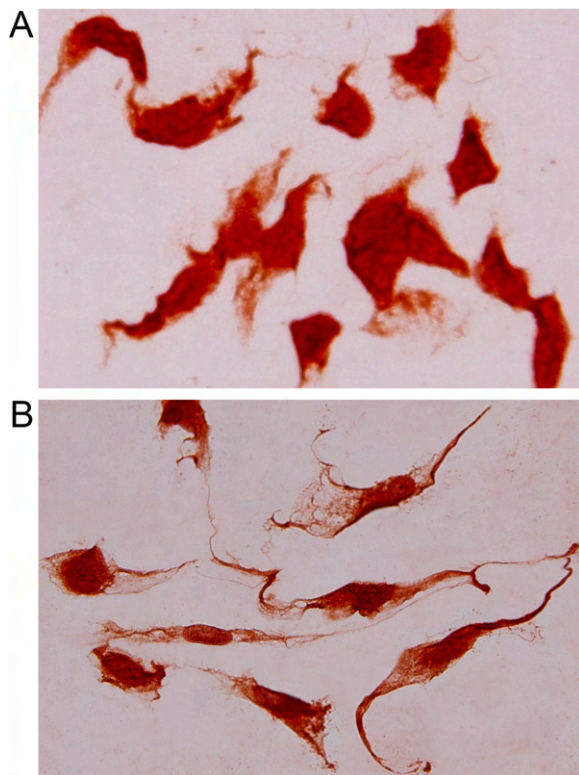


Fig. 8. Immunohistochemical staining for α -SMA and OPN in cultured stellate cells isolated from in rat liver. Stellate cells were isolated from rat liver and cultured for 7 days. (A) Staining for α -SMA to demonstrate that all the cultured and activated cells express α -SMA, which is a characteristic marker for stellate cells. (B) The cultured and activated stellate cells stained for OPN to demonstrate that stellate cells express OPN. This further proved that the increased source of OPN during hepatic fibrosis is expressed by activated stellate cells.

the hepatic parenchyma are the prominent characteristics of hepatic fibrosis. We have measured and evaluated the markers for most of the prominent characteristic features of hepatic fibrosis to study effect of EGCG treatment to arrest the pathogenesis and progression of hepatic fibrosis. Hematoxylin and Eosin staining of paraffin liver sections demonstrated that treatment with EGCG could significantly reduce

hepatic necrosis and retain the lobular architecture of liver along with marked decrease of transaminases. Azan trichrome staining depicted dramatic decrease of the deposition of fibrillar collagen in the hepatic parenchyma of EGCG treated animals. Similarly, the total hepatic collagen content measured in terms hydroxyproline, the molecular fingerprint for collagen, demonstrated a significant reduction after treatment with EGCG. Real-time qPCR for collagen type I and type III mRNA depicted marked decrease in EGCG treated samples. Furthermore, collagen type IV and hyaluronic acid, which are prominent serum markers of liver fibrosis have been decreased markedly in the animals treated with EGCG. It was reported that both in-vitro and in-vivo, EGCG inhibits OPN-dependant experimental liver injury and fibrosis [42]. All these data clearly indicate that EGCG could effectively prevent pathogenesis and progression of hepatic fibrosis and could be used as a therapeutic agent to arrest liver fibrosis.

Oxidative stress is a condition that reflects an imbalance between production and accumulation of reactive oxygen species (ROS) in cells and tissues and the ability of a cellular system to detoxify the reactive intermediates. Oxidative stress induced lipid peroxidation and the consequent generation of highly electrophilic aldehydes delineate a potential mechanism by which ROS can inflict cellular membrane damage. The aldehyde, 4-hydroxy-2-nonenal (4-HNE) is a major end-product of peroxidation of omega-6 unsaturated fatty acids such as linoleic acid and arachidonic acid [43]. It has 3 reactive groups consisting an aldehyde, a double-bond at carbon 2, and a hydroxyl group at carbon 4. The formation of excessive 4-HNE is considered as one of the most reliable biomarker of lipid peroxidation during liver injury [44]. We have observed a marked decrease of ascorbic acid and reduced glutathione levels in the liver tissue during NDMA administration [8, 25]. Furthermore, we have reported significantly reduced levels of glutathione in hepatic ischemia-reperfusion injury in rats [45]. The marked diminish of cellular antioxidant status during toxic liver injury may be effectively restored by EGCG, which could be the reason for the mechanism of inhibition of hepatic fibrosis. In the present study, immunohistochemical staining for 4-HNE demonstrated that treatment with EGCG remarkably reduced ROS production and subsequent cellular membrane lipid peroxidation. Overall, the current data indicates that EGCG could effectively prevent the formation of 4-HNE, which play a significant role in the pathogenesis and progression of liver diseases.

One of the major reasons for hepatic cellular injury, tissue inflammation, and fibrosis is oxidative stress that cause series of impairments including cellular membrane lipids. Under normal physiological conditions low rates of lipid peroxidation occurs, which stimulates cellular maintenance and survival through constitutive antioxidant defense mechanisms and signaling pathways as an adaptive stress response. Excessive production of ROS and subsequent cellular oxidative stress leads to enhanced lipid peroxidation that forms a variety of reactive aldehydes. Malondialdehyde is an end product of lipid peroxidation of polyunsaturated fatty acids and one of the best markers of ROS and oxidative stress [46]. It is a highly reactive compound and mutagen that can form nucleic acid and protein adducts. The protein adducts formed from MDA are referred as advanced lipoxidation end-products (ALEs) analogous to advanced glycation end-products (AGEs) [47]. Since enhanced lipid peroxidation and increased production of MDA triggers pathogenesis of hepatic fibrosis, it is important to prevent cellular oxidative stress and subsequent membrane damage. In the current study, we have observed a marked reduction in plasma MDA levels in EGCG treated animals indicating EGCG is capable to prevent excessive generation of ROS and subsequent cellular oxidative stress. This is in par with the report of a powerful hepatoprotective effect of EGCG to mitigate liver injury and toxicity induced by diethylnitrosamine [48].

When there is a chronic stimulus such as regular alcohol intake or infection with a virus, the round quiescent hepatic stellate cells will get activated and transformed into myofibroblast like cells with the expression of α -smooth muscle actin filaments [12]. This process is accompanied with the production of numerous cytokines and growth

factors and upregulation of the expression of numerous connective tissue proteins including OPN [26,49]. The activation and trans-differentiation of quiescent hepatic stellate cells is a result of a complex interplay between the parenchymal cells, dendritic cells, and extracellular matrix milieu and is a major rate limiting event in the pathogenesis of hepatic fibrosis [50]. In the current study we observed extensive and remarkable activation of hepatic stellate cells in NDMA treated animals. On the other hand, in EGCG treated animals, the activation hepatic stellate cells were very minimum and negligible. This data clearly indicates that EGCG can effectively prevent activation and transformation hepatic stellate cells and subsequent enhanced synthesis of connective tissue components. Furthermore, qPCR for α -SMA, a characteristic marker for activated stellate cells, depicted significant decrease of mRNA levels in the liver tissue of EGCG treated animals.

The activation and transformation of hepatic stellate cells is accompanied with upregulation of numerous connective proteins including OPN. In the present study we stained activated stellate cells for OPN to demonstrate that stellate cells express OPN during pathogenesis of hepatic fibrosis. An interesting feature of the activated hepatic stellate cells both in-vitro and in-vivo is to intricate and cross-talk with adjacent cells. This phenomena is clearly evident in cultured hepatic stellate cells in the current study (Fig. 8B). Every activated stellate cell in the image was interlocked with another cell in some place. The crosstalk between activated stellate cells and with other non-parenchymal cells including sinusoidal endothelial cells, bile duct epithelial cells, platelets, hepatic macrophages (Kupffer cells), natural killer cells, or dendritic cells either directly or indirectly contributes to form a cellular microenvironment and promotes the pathogenesis and progression of hepatic fibrosis [51]. In the current study, staining of cultured and activated primary hepatic stellate cells from rat liver provided evidence that stellate cells express OPN during the pathogenesis of hepatic fibrosis. Therefore, finding appropriate strategies to inhibit activation and transformation of quiescent hepatic stellate cells could prevent hepatic fibrosis, subsequent liver cirrhosis, hepatocellular carcinoma, and ultimate death.

In conclusion, the results of the present study demonstrated that treatment with EGCG can effectively prevent excessive generation of free radicals, cellular oxidative stress, hepatic inflammation, and upregulation OPN. Furthermore, EGCG inhibits activation of hepatic stellate cells, decreases expression of hyaluronic acid, and prevents deposition of collagen fibers in the extracellular matrix of liver. Overall, the data indicate that EGCG could be used as a potent therapeutic agent to prevent pathogenesis of hepatic fibrosis and subsequent adverse events such as liver cirrhosis and hepatocellular carcinoma.

Ethics approval

The animal experiments protocol (# 2012-47) was approved by the Animal Care and Use Committee of Kanazawa Medical University on the Ethics in the care and use of experimental animals.

Data Availability

The data will be available for verification upon request.

CRediT authorship contribution statement

J. George carried out all the major experiments, collected and analyzed the data, and wrote the manuscript. M. Tsuchishima provided technical and material support. M. Tsutsumi involved in conception and design of the study and obtained funding.

Funding

This work was supported in part by Grant for Specially Promoted Research from Kanazawa Medical University, Japan (Grant #SR 2012-04) to M. Tsutsumi.

Conflict of interest statement

The authors do not have any conflicts of interest to declare in connection with this manuscript.

Data Availability

Data will be made available on request.

Acknowledgements

The authors are thankful to Mr. Mitsuru Araya for his technical assistance and support in the animal experiments.

References

- [1] P. Acharya, K. Chouhan, S. Weiskirchen, R. Weiskirchen, Cellular mechanisms of liver fibrosis, *Front. Pharmacol.* 12 (2021), 671640, <https://doi.org/10.3389/fphar.2021.671640>.
- [2] J. George, K.R. Rao, R. Stern, G. Chandrakasan, Dimethylnitrosamine-induced liver injury in rats: the early deposition of collagen, *Toxicology* 156 (2–3) (2001) 129–138, [https://doi.org/10.1016/S0300-483X\(00\)00352-8](https://doi.org/10.1016/S0300-483X(00)00352-8).
- [3] J. George, G. Chandrakasan, Molecular characteristics of dimethylnitrosamine induced fibrotic liver collagen, *Biochim. Biophys. Acta* 1292 (2) (1996) 215–222, [https://doi.org/10.1016/0167-4838\(95\)00202-2](https://doi.org/10.1016/0167-4838(95)00202-2).
- [4] E. Mormone, J. George, N. Nieto, Molecular pathogenesis of hepatic fibrosis and current therapeutic approaches, *Chem. Biol. Interface* 193 (3) (2011) 225–231, <https://doi.org/10.1016/j.cbi.2011.07.001>.
- [5] T. Minato, M. Tsutsumi, M. Tsuchishima, N. Hayashi, T. Saito, Y. Matsue, N. Toshikuni, T. Arisawa, J. George, Binge alcohol consumption aggravates oxidative stress and promotes pathogenesis of NASH from obesity-induced simple steatosis, *Mol. Med.* 20 (1) (2014) 490–502, <https://doi.org/10.2119/molmed.2014.00048>.
- [6] J. George, Determination of selenium during pathogenesis of hepatic fibrosis employing hydride generation and inductively coupled plasma mass spectrometry, *Biol. Chem.* 399 (5) (2018) 499–509, <https://doi.org/10.1515/hsz-2017-0260>.
- [7] J. George, Elevated serum beta-glucuronidase reflects hepatic lysosomal fragility following toxic liver injury in rats, *Biochem. Cell Biol.* 86 (3) (2008) 235–243, <https://doi.org/10.1139/o08-038>.
- [8] J. George, Ascorbic acid concentrations in dimethylnitrosamine-induced hepatic fibrosis in rats, *Clin. Chim. Acta* 335 (1–2) (2003) 39–47, [https://doi.org/10.1016/S0009-8981\(03\)00285-7](https://doi.org/10.1016/S0009-8981(03)00285-7).
- [9] J. Cai, M. Hu, Z. Chen, Z. Ling, The roles and mechanisms of hypoxia in liver fibrosis, *J. Transl. Med.* 19 (1) (2021) 186, <https://doi.org/10.1186/s12967-021-02854-x>.
- [10] R. Kubota, N. Hayashi, K. Kinoshita, T. Saito, K. Ozaki, Y. Ueda, M. Tsuchishima, M. Tsutsumi, J. George, Inhibition of γ -glutamyltransferase ameliorates ischaemia-reoxygenation tissue damage in rats with hepatic steatosis, *Br. J. Pharmacol.* 177 (22) (2020) 5195–5207, <https://doi.org/10.1111/bph.15258>.
- [11] J. George, M. Tsutsumi, M. Tsuchishima, MMP-13 deletion decreases profibrogenic molecules and attenuates N-nitrosodimethylamine-induced liver injury and fibrosis in mice, *J. Cell. Mol. Med.* 21 (12) (2017) 3821–3835, <https://doi.org/10.1111/jcmm.13304>.
- [12] J. George, M. Tsutsumi, siRNA-mediated knockdown of connective tissue growth factor prevents N-nitrosodimethylamine-induced hepatic fibrosis in rats, *Gene Ther.* 14 (10) (2007) 790–803, <https://doi.org/10.1038/sj.gt.3302929>.
- [13] J. George, M. Tsutsumi, S. Takase, Expression of hyaluronic acid in N-nitrosodimethylamine induced hepatic fibrosis in rats, *Int. J. Biochem. Cell Biol.* 36 (2) (2004) 307–319, [https://doi.org/10.1016/S1357-2725\(03\)00253-x](https://doi.org/10.1016/S1357-2725(03)00253-x).
- [14] J. George, G. Chandrakasan, Glycoprotein metabolism in dimethylnitrosamine induced hepatic fibrosis in rats, *Int. J. Biochem. Cell Biol.* 28 (3) (1996) 353–361, [https://doi.org/10.1016/1357-2725\(95\)00140-9](https://doi.org/10.1016/1357-2725(95)00140-9).
- [15] A. Oldberg, A. Franzén, D. Heinegård, Cloning and sequence analysis of rat bone sialoprotein (osteopontin) cDNA reveals an Arg-Gly-Asp cell-binding sequence, *Proc. Natl. Acad. Sci. USA* 83 (23) (1986) 8819–8823, <https://doi.org/10.1073/pnas.83.23.8819>.
- [16] S.A. Lund, C.M. Giachelli, M. Scatena, The role of osteopontin in inflammatory processes, *J. Cell Commun. Signal.* 3 (3–4) (2009) 311–322, <https://doi.org/10.1007/s12079-009-0068-0>.
- [17] M.A. Icer, M. Gezmen-Karadag, The multiple functions and mechanisms of osteopontin, *Clin. Biochem.* 59 (2018) 17–24, <https://doi.org/10.1016/j.clinbiochem.2018.07.003>.
- [18] S. Nagoshi, Osteopontin: Versatile modulator of liver diseases, *Hepatol. Res.* 44 (1) (2014) 22–30, <https://doi.org/10.1111/hepr.12166>.
- [19] R. Urtasun, A. Lopategi, J. George, T.M. Leung, Y. Lu, X. Wang, X. Ge, M.I. Fiel, Nieto N. Osteopontin, an oxidant stress sensitive cytokine, up-regulates collagen-I via integrin $\alpha(V)\beta(3)$ engagement and PI3K/pAkt/NF κ B signaling, *Hepatology* 55 (2) (2012) 594–608, <https://doi.org/10.1002/hep.24701>.
- [20] Y. Matsue, M. Tsutsumi, N. Hayashi, T. Saito, M. Tsuchishima, N. Toshikuni, T. Arisawa, J. George, Serum osteopontin predicts degree of hepatic fibrosis and

- serves as a biomarker in patients with hepatitis C virus infection, *PLoS One* 10 (3) (2015), e0118744, <https://doi.org/10.1371/journal.pone.0118744>.
- [21] B.N. Singh, S. Shankar, R.K. Srivastava, Green tea catechin, epigallocatechin-3-gallate (EGCG): mechanisms, perspectives and clinical applications, *Biochem. Pharmacol.* 82 (12) (2011) 1807–1821, <https://doi.org/10.1016/j.bcp.2011.07.093>.
- [22] Y. Ding, X. Sun, Y. Chen, Y. Deng, K. Qian, Epigallocatechin gallate attenuated non-alcoholic steatohepatitis induced by methionine- and choline-deficient diet, *Eur. J. Pharmacol.* 761 (2015) 405–412, <https://doi.org/10.1016/j.ejphar.2015.05.005>.
- [23] E. Tak, G.C. Park, S.H. Kim, D.Y. Jun, J. Lee, S. Hwang, G.W. Song, S.G. Lee, Epigallocatechin-3-gallate protects against hepatic ischaemia-reperfusion injury by reducing oxidative stress and apoptotic cell death, *J. Int. Med. Res.* 44 (6) (2016) 1248–1262, <https://doi.org/10.1177/0300060516662735>.
- [24] J. George, G. Chandrakasan, Biochemical abnormalities during the progression of hepatic fibrosis induced by dimethylnitrosamine, *Clin. Biochem.* 33 (7) (2000) 563–570, [https://doi.org/10.1016/s0009-9120\(00\)00170-3](https://doi.org/10.1016/s0009-9120(00)00170-3).
- [25] J. George, M. Tsutsumi, M. Tsuchishima, Alteration of trace elements during pathogenesis of N-nitrosodimethylamine induced hepatic fibrosis, *Sci. Rep.* 9 (2019) 708, <https://doi.org/10.1038/s41598-018-37516-4>.
- [26] J. George, M. Tsuchishima, M. Tsutsumi, Molecular mechanisms in the pathogenesis of N-nitrosodimethylamine induced hepatic fibrosis, *Cell Death Dis.* 10 (1) (2019) 18, <https://doi.org/10.1038/s41419-018-1272-8>.
- [27] J. George, M. Tsuchishima, M. Tsutsumi, Metabolism of N-nitrosodimethylamine, methylation of macromolecules, and development of hepatic fibrosis in rodent models, *J. Mol. Med.* 98 (9) (2020) 1203–1213, <https://doi.org/10.1007/s00109-020-01950-7>.
- [28] J. George, G. Chandrakasan, Biochemical abnormalities during the progression of hepatic fibrosis induced by dimethylnitrosamine, *Clin. Biochem.* 33 (7) (2000) 563–570, [https://doi.org/10.1016/s0009-9120\(00\)00170-3](https://doi.org/10.1016/s0009-9120(00)00170-3).
- [29] J. George, G. Chandrakasan, Lactate dehydrogenase isoenzymes in dimethylnitrosamine induced hepatic fibrosis, *J. Clin. Biochem. Nutr.* 22 (1) (1997) 51–62, <https://doi.org/10.3164/jcbs.22.51>.
- [30] J. George, R. Stern, Serum hyaluronan and hyaluronidase: very early markers of toxic liver injury, *Clin. Chim. Acta* 348 (1–2) (2004) 189–197, <https://doi.org/10.1016/j.cccn.2004.05.018>.
- [31] J. George, Mineral metabolism in dimethylnitrosamine-induced hepatic fibrosis, *Clin. Biochem.* 39 (10) (2006) 984–991, <https://doi.org/10.1016/j.clinbiochem.2006.07.002>.
- [32] B. Ramachandran, S. Jayavelu, K. Murhekar, T. Rajkumar, Repeated dose studies with pure Epigallocatechin-3-gallate demonstrated dose and route dependant hepatotoxicity with associated dyslipidemia, *Toxicol. Rep.* 3 (2016) 336–345, <https://doi.org/10.1016/j.toxrep.2016.03.001>.
- [33] C.H. Li, D.M. Piao, W.X. Xu, Z.R. Yin, J.S. Jin, Z.S. Shen, Morphological and serum hyaluronic acid, laminin and type IV collagen changes in dimethylnitrosamine-induced hepatic fibrosis of rats, *World J. Gastroenterol.* 11 (48) (2005) 7620–7624, <https://doi.org/10.3748/wjg.v11.i48.7620>.
- [34] Y. Hirakawa, M. Tsuchishima, A. Fukumura, K. Kinoshita, N. Hayashi, T. Saito, J. George, N. Toshiyuki, Y. Ueda, M. Tsutsumi, Recombinant thrombomodulin prevented hepatic ischemia-reperfusion injury by inhibiting high-mobility group box 1 in rats, *Eur. J. Pharmacol.* 863 (2019), 172681, <https://doi.org/10.1016/j.ejphar.2019.172681>.
- [35] G. Tang, Y. Xu, C. Zhang, N. Wang, H. Li, Y. Feng, Green Tea and Epigallocatechin Gallate (EGCG) for the management of Nonalcoholic Fatty Liver Diseases (NAFLD): insights into the role of oxidative stress and antioxidant mechanism, *Antioxidants* 10 (7) (2021) 1076, <https://doi.org/10.3390/antiox10071076>.
- [36] Q.P. Dou, Molecular mechanisms of green tea polyphenols, *Nutr. Cancer* 61 (6) (2009) 827–835, <https://doi.org/10.1080/01635580903285049>.
- [37] J. Hu, D. Webster, J. Cao, A. Shao, The safety of green tea and green tea extract consumption in adults - results of a systematic review, *Regul. Toxicol. Pharmacol.* 95 (2018) 412–433, <https://doi.org/10.1016/j.yrtph.2018.03.019>.
- [38] L.M. Castello, D. Raineri, L. Salmi, N. Clemente, R. Vaschetto, M. Quaglia, M. Garzaro, S. Gentili, P. Navalesi, V. Cantaluppi, U. Dianzani, A. Aspesi, A. Chiochetti, Osteopontin at the crossroads of inflammation and tumor progression, *Mediat. Inflamm.* 2017 (2017) 4049098, <https://doi.org/10.1155/2017/4049098>.
- [39] S.I. Liochev, Reactive oxygen species and the free radical theory of aging, *Free Radic. Biol. Med.* 60 (2013) 1–4, <https://doi.org/10.1016/j.freeradbiomed.2013.02.011>.
- [40] J. George, Metabolism and interactions of antileprosy drugs, *Biochem. Pharmacol.* 177 (2020), 113993, <https://doi.org/10.1016/j.bcp.2020.113993>.
- [41] Hryciay EG, Bandiera SM. Involvement of cytochrome P450 in reactive oxygen species formation and cancer. In: *Advances in Pharmacology* Vol. 74, 2015; pp. 35–84. Edited by Hardwick JP. (<https://doi.org/10.1016/bs.apha.2015.03.003>).
- [42] M.L. Arffa, M.A. Zapf, A.N. Kothari, V. Chang, G.N. Gupta, X. Ding, M.M. Al-Gayyar, W. Syn, N.M. Elsherbiny, P.C. Kuo, Z. Mi, Epigallocatechin-3-gallate upregulates miR-221 to inhibit osteopontin-dependent hepatic fibrosis, *PLoS One* 11 (12) (2016), e0167435, <https://doi.org/10.1371/journal.pone.0167435>.
- [43] A. Ayala, M.F. Muñoz, S. Argüelles, Lipid peroxidation: production, metabolism, and signaling mechanisms of malondialdehyde and 4-hydroxy-2-nonenal, *Oxid. Med. Cell. Longev.* 2014 (2014), 360438, <https://doi.org/10.1155/2014/360438>.
- [44] G. Poli, F. Biasi, G. Leonarduzzi, 4-Hydroxynonenal-protein adducts: a reliable biomarker of lipid oxidation in liver diseases, *Mol. Asp. Med.* 29 (1–2) (2008) 67–71, <https://doi.org/10.1016/j.mam.2007.09.016>.
- [45] K. Tamura, N. Hayashi, J. George, N. Toshiyuki, T. Arisawa, J. Hiratake, M. Tsuchishima, M. Tsutsumi, GGsTop, a novel and specific γ -glutamyl transpeptidase inhibitor, protects hepatic ischemia-reperfusion injury in rats, *Am. J. Physiol. Gastrointest. Liver Physiol.* 311 (2) (2016) G305–G312, <https://doi.org/10.1152/ajpgi.00439.2015>.
- [46] D. Del Rio, A.J. Stewart, N. Pellegrini, A review of recent studies on malondialdehyde as toxic molecule and biological marker of oxidative stress, *Nutr. Metab. Cardiovasc. Dis.* 15 (4) (2005) 316–328, <https://doi.org/10.1016/j.numecd.2005.05.003>.
- [47] N.T. Moldogazieva, I.M. Mokhosoev, T.I. Mel'nikova, Y.B. Porozov, A.A. Terentiev, Oxidative stress and advanced lipoxidation and glycation end products (ALEs and AGEs) in aging and age-related diseases, *Oxid. Med. Cell. Longev.* 2019 (2019) 3085756, <https://doi.org/10.1155/2019/3085756>.
- [48] S.A. Almatroodi, M.A. Alsalhi, H.M. Alharbi, A.A. Khan, A.H. Rahmani, Epigallocatechin-3-gallate (E.G.C.G.), an active constituent of green tea: implications in the prevention of liver injury induced by diethylnitrosamine (DEN) in rats, *Appl. Sci.* 9 (22) (2019) 4821, <https://doi.org/10.3390/app9224821>.
- [49] C.Y. Zhang, W.G. Yuan, P. He, J.H. Lei, C.X. Wang, Liver fibrosis and hepatic stellate cells: Etiology, pathological hallmarks and therapeutic targets, *World J. Gastroenterol.* 22 (48) (2016) 10512–10522, <https://doi.org/10.3748/wjg.v22.i48.10512>.
- [50] T. Tsuchida, S.L. Friedman, Mechanisms of hepatic stellate cell activation, *Nat. Rev. Gastroenterol. Hepatol.* 14 (7) (2017) 397–411, <https://doi.org/10.1038/nrgastro.2017.38>.
- [51] F. Yang, H. Li, Y. Li, Y. Hao, C. Wang, P. Jia, X. Chen, S. Ma, Z. Xiao, Crosstalk between hepatic stellate cells and surrounding cells in hepatic fibrosis, *Int. Immunopharmacol.* 99 (2021), 108051, <https://doi.org/10.1016/j.intimp.2021.108051>.